

# The Status of Natural Radioactivity and Heavy Metals Pollution on Marine Sediments Red Sea Coast, At Safaga, Egypt

M. A. M. UOSIF\*<sup>1</sup>, SHAMS.ISSA<sup>1,3</sup>, HESHAM M.H. ZAKALY<sup>1</sup>, MADKOUR. HASHIM<sup>2</sup>, AND MAHMOUD TAMAM<sup>1</sup>

<sup>1</sup>Faculty of Science, Al-Azhar University, Assuit branch, Egypt

<sup>2</sup>National Institute of Oceanography and Fisheries, Hurghada, Egypt

<sup>3</sup>Faculty of Science, Tabok University, Tabok, Saudi Arabia

**Email:** dr\_mohamed\_amin@lycos.com

Received: September 15, 2015 | Revised: December 08, 2015 | Accepted: January 17, 2016

Published online: February 08, 2016, The Author(s) 2016. This article is published with open access at [www.chitkara.edu.in/publications](http://www.chitkara.edu.in/publications)

**Abstract:** Natural <sup>226</sup>Ra, <sup>232</sup>Th and <sup>40</sup>K radio nuclides concentration in beach Sediments along Safaga coast of Red sea, Egypt has been carried out using a NaI (Tl) gamma ray spectrometric technique. The total average concentrations of radionuclides  $\pm$  uncertainty of <sup>226</sup>Ra, <sup>232</sup>Th and <sup>40</sup>K were  $22.2 \pm 1.7$ ,  $19.2 \pm 2.5$ , and  $477.6 \pm 27.6$  Bq kg<sup>-1</sup>, respectively. The total average absorbed dose rate is found to be 41.4 nGyh<sup>-1</sup>, whereas the annual effective dose rate has an average value of 54  $\mu$ Svy<sup>-1</sup>. The total organic matter (TOC), carbonates (CaCo<sub>3</sub>) and Heavy metals distribution have been measured at some locations, the concentration for the investigated heavy metals overtake the allowable limits recommended by the Canadian Environmental Quality Guidelines, this assigned to the ratio of metals pollution is caused by anthropogenic activities (phosphate shipment as in Abu Tartour harbor and navigation as in Touristic harbor) and or by natural impacts such in mangrove interment. Statistical analyses were carried out between the parameters obtained from the radioactivity to know the existing relations and to study the spatial distribution of radionuclide.

**Keywords:** radiation hazard; radionuclides; natural radioactivity; Heavy metals ; Safaga; Red Sea; Egypt; marine sediments.

## 1. INTRODUCTION

The Egyptian Red Sea coast is being stressed due to over exploitation and has become very vulnerable to human related activities. Generally, the main

Journal of Nuclear  
Physics, Material  
Sciences, Radiation and  
Applications  
Vol-3, No-2  
February 2016  
pp. 191–222

---

Uosif, MAM  
Issa1, S  
Sharma, I  
Zakaly, HMM  
Hashim, M  
Tamam, M

---

environmental problems and threats to the Red Sea ecosystem and geosystem include recreation and tourism activities, landfilling, dredging, oil pollution, water pollution, solid waste disposal, navigation activities, phosphate shipment pollution and fishing activities. As a result of the human activities, pollution extends along the shore, and is discharged to the near shore waters. Some of these pollutants may directly or indirectly be captured by bottom sediments [1]. In the case of successive concentrations of these pollutants in bottom sediments, the later will act as a reservoir for pollutants. Therefore, studies of the recent sediments along the Red Sea coasts are important in estimating potential environmental hazards resulting from the illegitimate human activities.

The natural radionuclides of the uranium ( $^{238}\text{U}$ ) and thorium ( $^{232}\text{Th}$ ) series and  $^{40}\text{K}$  as well as the artificial radionuclides of  $^{137}\text{Cs}$ ,  $^{90}\text{Sr}$  and  $^{239+240}\text{Pu}$  are the major long-lived radionuclides already present or introduced into seas [2]. Thorium isotopes have been widely used as tracers for particle dynamics in marine geochemistry. Particle-reactive radionuclides are useful as particle transport tracers. All sizes of Particles play a central role in the scavenging of particle-reactive radionuclides and pollutants in embouchure, coastal and open oceans [3]. Documented that the environmental radiotracers can be used to understand the underlying processes of the environment where they are found. The presence of artificial radionuclides in the marine environment can thus lead to radiation exposure through the ingestion of sea food [4]. Investigators have reported a wide variation in the concentrations of uranium and radium in samples from various parts of the world. For uranium, a range from 3 to 400 ppm, corresponding to 37–4900 Bq  $^{238}\text{U kg}^{-1}$  (1 ppm U = 12.23 Bq  $^{238}\text{U kg}^{-1}$ ) and for  $^{226}\text{Ra}$ , a range from 100 to 10 000 Bq  $\text{kg}^{-1}$  is reported. It is within this context that the present study aimed to determination of the radioactivities of naturally occurring nuclides in marine sediment. [5].

Among the various geological formations, sediment plays a predominant role in aquatic radioecology and plays a role in accumulating and transporting contaminants within the geographic area. It is the basic indicator of radiological contamination in the environment [6]. Beach sediments are mineral deposits formed through weathering and erosion of either igneous or metamorphic rocks. Among the rock constituent minerals are some natural radionuclides that contribute to ionizing radiation exposure on Earth. Natural radioactivity in soils comes from U and Th series and natural K. The study of the distribution of primordial radionuclides allows the understanding of the radiological implication of these elements due to the gamma-ray exposure of the body and irradiation of lung tissue from inhalation of radon and its daughters [7].

---

---

The information about the radiological and geochemical pollution of marine sediments in Safaga (Egyptian Red Sea coast) is limited consequently, and need update to exam the status of natural radioactivity and heavy metals pollution in area under investigation. Beside that associated radiological hazards we calculating the absorbed dose rate, annual effective dose rate, representative level index and external hazard index. The data which obtained are fundamental to drawing a radiological map for Egyptian Red Sea coast

## 2. MATERIALS AND METHODS

### 2.1 Study regions

The study area *Safaga City* divided into three stations from south to north namely; Mangrove area (K17), Abu-Tartour Harbour and Touristic Harbour (Fig. 1).

**Station I: Mangrove area (k 17)**, it is located at latitude  $26^{\circ} 36' 56''$  N and longitude  $34^{\circ} 00' 43''$  E (Table 1 and Fig. 2-a). It is distinguished by mangrove trees (*Avicennia marina*) and tidal zone reach to about 100 m occupied by sand mud and small rocks, the tidal zone followed by deep water which begins with 5 m. There is successful transplantation operation carried out in this area by Egyptian Environmental Affairs Agency (EEAA).

**Station II: Abu-Tartour harbour**, it is located out of Safaga City. It is situated between latitude  $26^{\circ} 41' 46''$  N and longitude  $33^{\circ} 55' 47''$  E (Table 1 and Fig. 2-b). Its activities are limited to exporting of the Egyptian phosphate, packed cement and crude alchortz. Shoreward, the area is skirted by high basement mountains. The beach sediments are generally coarse sands mixed with common rock-forming detritus from the surrounding formations. The sediments covering the intertidal zone are fine to very fine sands sizes and rich in terrigenous constituents. On the other hand, bottom topography of Abu-Tartour Harbour is mud to sandy mud. This is due to phosphate shipment; packing of cement and other activities enter this harbour.

**Station III: Touristic Harbour**, it is located at north Safaga City. It is lying at latitude  $26^{\circ} 45' 98''$  N and longitude  $33^{\circ} 56' 42''$  E (Table 1 and Fig. 2-c). Generally, the northern part of the Red Sea is characterized by the existence of a wide intertidal zone (~1000m wide). Also, Shoreward, the area is skirted by a raised reefal limestone (about 1.0m in height) that is considered to have been deposited during the marine transgression in the late Pleistocene or early Holocene [8]. The Egyptian experts of egyptian environmental affairs agency (EEAA) and Danish experts studied this area then, the EEAA allowed to use landfilling and dredging on beach and intertidal zone during construction this

---

Uosif, MAM  
Issa1, S  
Sharma, I  
Zakaly, HMM  
Hashim, M  
Tamam, M

---

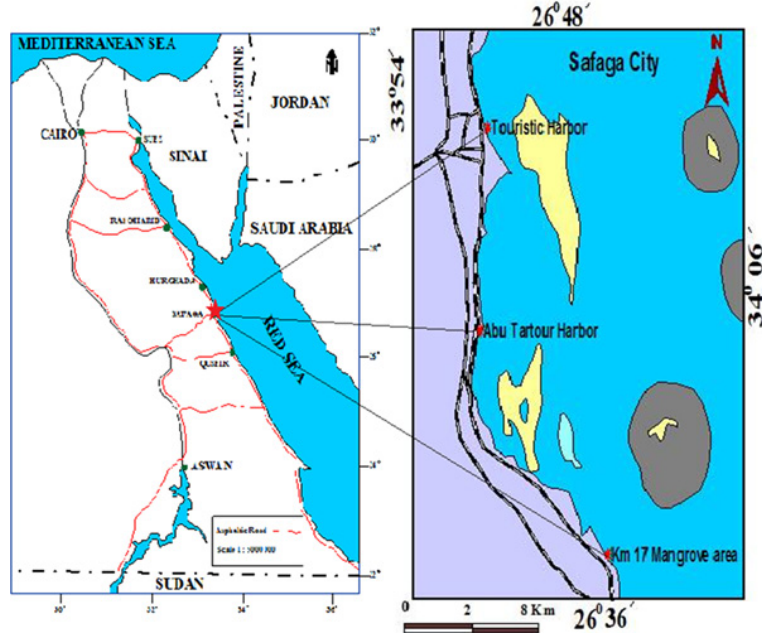


**Figure 1:** Map showing the location of the three areas were studied at Safaga and surrounding areas.

marina. A geotextile curtain has been used during the operation for preventing dust from spreading to the surrounding environment but in many times the wind was cut the geotextile. The fill operation has been used sediments transported from the natural land of this site, and mountain area, and as illustrated in the figures there are many solid wastes and disposal of garbage from the boats in addition to, sunken boats at the area. Patch reefs and fringing reefs characterize the area in front of Tourist Harbour. The most common and widely distributed coral species in this area are *Acropora* sp., and *Stylophora pistillata*. A long the intertidal zone, there are some patches of seagrass. Dense algal species and coralline algae are incorporated with the reefs.

## 2.2 Sample collection and preparation

Eighteen samples of sediment have been collected from Safaga city coastline, Red sea. Samples collection was considered the locations throughout three Stations (Km 17 Mangrove area, Abu Tartour Harbor and Touristic Harbor) in Safaga, Red sea governorate, Egypt, as shown in figure 1. six samples have been collected from Km 17 Mangrove area (south town), also 6 samples from Abu Tartour Harbor (Middle town) and 6 samples Touristic Harbor (North town)). Table 1.

---

**Table 1:** The hydrographic parameters of water mass in the studied areas.

Studied areas	position		Depth (m)	PH	Temp. (°C)	TDS (ppt)	s w s g ms\ (σt) cm	SPC ms\ cm	
	Lat. ° , “ N	Long. ° , “ E							
Km 17 Mangrove area		34° 0'43"	H1	0.5 8.8	43.6	14.6	32	33	64.5
			H2	0.3 8.7	43.8	15.9	32	32	63.9
		26°36'56"	H3	0.5 8.6	43.3	15.2	32	32	64
Abu-Tartour			H4	2.5 8.6	42.4	20.7	31	30	62.8
		33°55'47"	H5	1.5 8.6	42.3	20.6	31	30	62.7
			H6	4.0 8.8	42.9	21.2	31	30	62.7
Touristic Harbour			H7	0.3 8.8	42.9	23	32	30	63.5
		33° 56'42"	H8	0.3 8.6	42.4	21.8	31	30	62.8
		26° 45' 98"	H9	0.3 8.6	42.4	21.4	31	30	62.8

Density Functional Theory Study of Structural and Electronic Properties of Group V Transition Metal Carbide

Uosif, MAM  
Issa1, S  
Sharma, I  
Zakaly, HMM  
Hashim, M  
Tamam, M

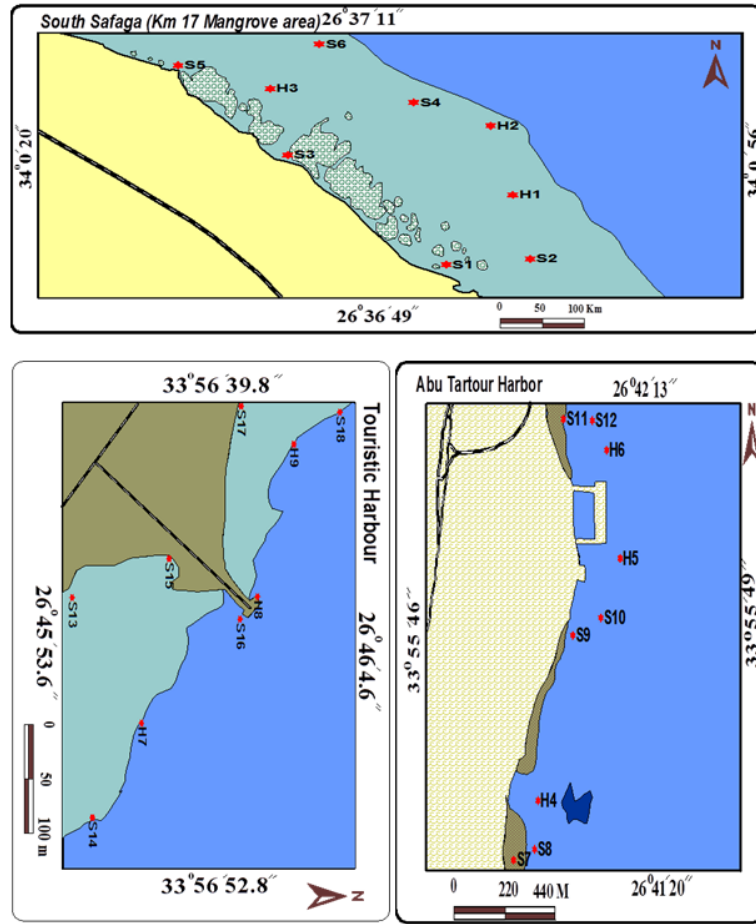


**Figure 2:** Samples Location in the Study area.

The locations (Co-Ordinates) were determined by using Geographical Position System GPS (Magellan). The physical criteria of water (temperature, salinity, pH, depth, specific conductivity (SPC) and total dissolved salts (TDS) were measured directly in the field using Hydrolab Instrument (HANNA HI 9828) during collecting of samples at the studied localities, See table 1.

The location and description of bottom characteristics of the collected samples are given in (Figures 2). Sediment samples were collected by hand, grab sampler and scuba diving. Three different environmental zones such as (i) beach, (ii) intertidal zone and (iii) offshore zone until 4 m water depth represent these localities. Scuba diving was used in areas rich in corals where grab sampler failed to collect samples.

### 2.3 Mechanical (Granulometric) Analysis

Electroformed sieves are now available that take the range of analysis below the 31  $\mu\text{m}$  permitted by woven-wire sieves. This has extended the range down to 5  $\mu\text{m}$ , but not for routine analysis [9]. About 100 gm of prepared sample were taken for mechanical analysis, which was carried out using a standard set of sieves, shacked in a Ro-Tap shaker for 20 minutes. The sieves were arranged where 1 $\Phi$  interval separates each sieve from another. The used sieves are 2.0, 1.0, 0.5, 0.25, 0.125 and 0.063 mm in addition to the ban. These sieves have the equivalent -1, 0, 1, 2, 3 and 4  $\Phi$  values, respectively. The collected sieve fractions were accurately weighed. Each ban fraction weighing more than 5% of the analyzed sample was analyzed for silt and clay using the pipette method [10].

### 2.4 Geochemical Analysis

In the National Institute of Oceanography and Fisheries. Chemical and Geochemical analysis were carried out. Samples for geochemical analysis were produced by splitting the dry samples. Ten grams of each prepared subsamples of all collected samples were ground using an agate mortar (Retsch Mortar-method), passed through a 80 mesh sieve and kept in dry, clean bag waiting for analysis.

- (1) **For total carbonates**, To determine the carbonate content, one gram of each prepared sample were treated by (1N HCL acid), filtered and washed several times by distilled water, dried and reweight in order to calculate the percentage of carbonate content of the sediments.
- (2) **For organic carbon and total organic matter**, One gram of each crude sample was burned to 550 °C for about two hours. The organic matter content of the sediments was determined by sequential weight loss at 550 °C [11-13].
- (3) **For heavy metals**, about 0.5 gm of well homogenized ground sediment samples were accurately weighed on an analytical balance and then transferred into a Teflon beaker and then were completely digested by using a mixture of concentration. Nitric, per chloric and hydrofluoric acids, with the ratio 3: 2: 1 respectively according to [14]. Acids were slowly added to dried sample and left overnight before heating. Samples were heated for two hours on hot plate at temperature of approximately 200 °C, then left to cool and filtered to get rid of the nondigested parts. The solution was justified to volume of 25 ml, and then the concentration of the elements was determined by Atomic Absorption Spectrophotometry (AAS). technique, using GBC-932 ver. 1.1 with detection limits 0.01 ppm

---

Uosif, MAM  
Issa1, S  
Sharma, I  
Zakaly, HMH  
Hashim, M  
Tamam, M

of the National Institute of Oceanography and Fisheries, Red Sea Branch.  
Results were expressed in ppm.

## 2.5 Gamma Spectroscopic Analysis

### 2.5.1 Sample preparation

The samples were prepared as follows. Each sample (about 1 kg) was washed in distilled water and dried at about 110°C to ensure that moisture is completely removed. The samples were crushed, homogenized and sieved through a 200 mesh, the optimum size to be enriched in heavy minerals. Weighted samples were placed in a polyethylene beaker of 350 cm<sup>3</sup> volume. The beakers were completely sealed for 4 weeks to reach secular equilibrium where the rate of decay of the progeny becomes equal to that of the parent (radium and thorium) [15]. This step is necessary to ensure that radon gas confined within the volume and the progeny will also remain in the sample.

### 2.6 Instrumentation and calibration

Radioactivity measurements were performed by gamma ray spectrometer, employing a scintillation detector 3 × 3 inch. Its hermetically sealed assembly which includes a high-resolution NaI (Tl) crystal, photomultiplier tube, an internal magnetic/light shield, aluminum housing and a 14 pin connector coupled to PC-MCA Canberra Accuspes. It has the following specifications: resolution 7.5% specified at the 662 keV peak of <sup>137</sup>Cs, window aluminum 0.5 mm thick, density 147 mg/cm<sup>2</sup>, reflector oxide; 1.6 mm thick; density 88 mg/cm<sup>2</sup>, magnetic/light shield-conetic lined steel and operating voltage positive 902 V (dc). To reduce gamma ray background, a cylindrical lead shield with a fixed bottom and movable cover shielded the detector. The lead shield contained an inner concentric cylinder of copper (0.3 mm thick). The detection array was energy calibrated using <sup>60</sup>Co (1173.2 and 1332.5 keV), <sup>133</sup>Ba (356.1 keV) and <sup>137</sup>Cs (661.9 keV), however, the efficiency calibration was made by calibration cylindrical beaker standard source *IAEA-314* [16], where the specific activity was known, which containing three radionuclides: <sup>226</sup>Ra, <sup>232</sup>Th and <sup>238</sup>U.

The offline analysis of each measured  $\gamma$ -ray spectrum has been carried out by a dedicated software program genie 2000 [17]. The <sup>226</sup>Ra radionuclide was estimated from the 351.9 keV  $\gamma$ -peak of <sup>214</sup>Pb, and 609.3 keV, 1120.3 keV, 1728.6 keV and 1764 keV  $\gamma$ -peak of <sup>214</sup>Bi. The 186 keV photon peak of <sup>226</sup>Ra was not used because of the interfering peak of <sup>235</sup>U, with energy of 185.7 keV. The <sup>232</sup>Th radionuclide was estimated from the 911.2 keV  $\gamma$ -peak of <sup>228</sup>Ac and the 238.6 keV  $\gamma$ -peak of <sup>212</sup>Pb. The <sup>40</sup>K radionuclide was estimated using the 1461 keV  $\gamma$ -peak from <sup>40</sup>K itself [18].

### 3. RESULTS AND DISCUSSION

#### 3.1 Environmental conditions

Oceanographic conditions spread along the shore have an exchangeable effect on the coastal features. The oceanographic parameters affect the shore environment and the same time have an impact on the shore activities. Most oceanographic parameters were measured at the study areas listed in (Table 1). The salinity of seawater in Mangrove region is high and varies between 43.3‰ at depth 0.5m and 43.8‰ at depth 0.3 m. The water temperature ranges between 15.2 °C at depth 0.5m and 15.9°C at depth 0.3m in the winter season, Jan.,2012 (period of collecting samples ) (Table 1). The salinity of seawater in Abu-Tartour harbore ranges between 42.3‰ at depth 1.5m and 43.9 at depth 4 m, and the water temperatures are between 20.6°C at depth 1.5m and 21.2°C at depth 4m in the winter season (Table 1). The salinity of water in Touristic Harbour is varies between 42.4 ‰ at depth 0.3m and 42.9 ‰ at depth 0.3 m, while the water temperatures are between 21.4 °C at depth 0.3m and 23 °C at depth 0.3m in the winter season (Table 1).

#### 3.2 Sediment texture

The purpose of such mechanical analysis of the sediment not just for the nature of the sediment, also to understand the physical properties of the sediments and revealed the relationship and the effect of the grain size, source materials and depositional environment.

Sediments of the investigated marine harbor and intertidal bottoms facies are composed of over 98% sand figure (3) table (2). Very fine sand and medium sand are the most dominant the beach sediments, whereas coarse sand and very coarse sand are the most abundant fractions in the intertidal sediment figure (3). Gravel is common in the intertidal samples and reach up to 34% with an average of 7% especially in Abu Tartour Harbor and in north (Touristic Harbour) reach up to 21% with average of 7% but in Mangrove area reach up to 23% with average 10%. Mud is relatively higher in the beach samples than in the intertidal sediments at Mangrove area. The areal distribution of sediments and the variation of their grain characteristic are controlled to a great extent by the nature of the coastal sediments, bottom facies and hydrodynamic status along the coast [19].

#### 3.3 Geochemistry

##### 3.3.1 Carbonates(CaCO<sub>3</sub>)

The average carbonates content in the investigated sediments varies from 7 % at Touristic Harbor in the north to 91 % at Mangrove area (Table, 2: Fig. 4).

Uosif, MAM  
 Issa1, S  
 Sharma, I  
 Zakaly, HMM  
 Hashim, M  
 Tamam, M

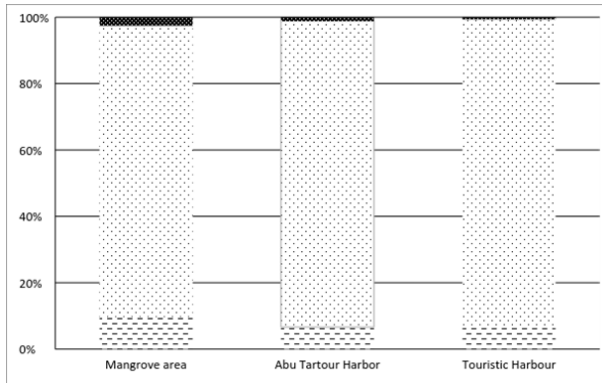


**Figure 3:** Distribution of gravel, sand and mud fractions of the sediment samples at the studied Regions.

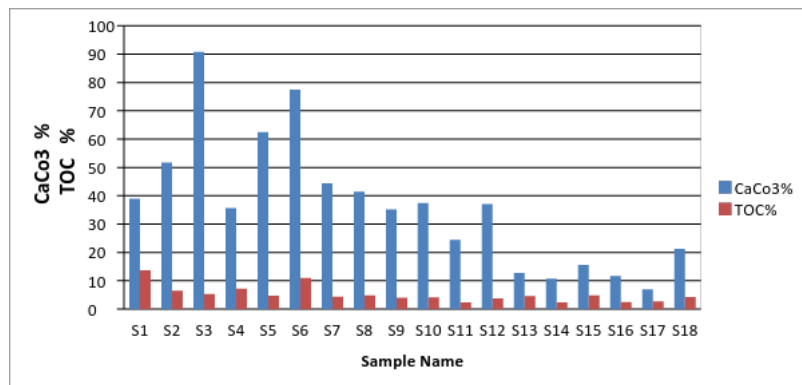


**Figure 4:** Distribution of carbonate content, total organic matter of marine sediments of Safaga City.

Mangrove area recorded the highest values of carbonate contents compared with the other studied areas. It is due to mangrove trees (*Avicennia marina*). On other hand, The four principal sources of carbonate in marine sediment are [20]:

1. Inorganic chemical precipitation.
2. Residual from weathering of limestone rock on the sea floor.
3. Terrestrial rock. and
4. Biogenic from accumulation of skeletal grains.

### 3.3.2 Total organic matter (TOC)

Organic matter affects the aquatic ecosystem by interacting with in organic matter to form complex compounds, which include in its structure several

other elements. It also serves as a source of food for sundry animal groups [21]. The content of organic matter in intertidal sediment varies from 2.3 % at Touristic Harbour to 13.7 % at Mangrove area (Table 2; Fig. 4). Mangrove area and Abu Tartour Harbor recorded the highest values of organic matter content compared with Touristic Harbour. The aerial distribution of the organic matter shown a general decrease toward the north.[22,23] attributed the high content of the organic matter in tidal flat sediments to the terrigenous influx. Also, they recorded that the terrestrial materials rich in organic matter and the high organic productivity are the two main reasons for the higher organic matter content.

**Table 2:** Sediment types, geochemical properties and heavy metals of sediment samples at the study areas.

Variables	South (Mangrove area) (n* = 6)		Middle (Abu Tartour Harbor) (n* = 6)		North (Touristic Harbour) (n (n*= 6)	
	Range (%)	Avg. (%)	Range (%)	Avg. (%)	Range (%)	Avg. (%)
Gravel	2–23	9.7	0–34	6.6	00.–21	6.9
Sand	77–96	87.7	65–98	92.2	79–98	92.4
Mud	1–8	2.6	1–2	1.2	0–3	0.7
Carb. %	36–91	59.6	24–44	36.7	7–21	13.2
TOM%	5–14	8.1	2–5	3.9	2–5	3.5
Fe**	64720–76277	70499	78589– 90146	84367	92457– 104014	98236
Mn**	378–531	445	281–578	373	200– 620	398
Zn**	38–53	45	52–117	76	40–361	117
Cu**	10–15	13	10–22	14	10–756	138
Pb**	7–24	16	4–28	15	22–81	37
Ni**	5–15	11	1–12	6	0–5	3
Cd**	0–0.4	0.1	0–1.2	0.6	0–0.8	0.2

Notes: n\*, number of samples; \*\*Values in  $\mu\text{g g}^{-1}$

Uosif, MAM  
 Issa1, S  
 Sharma, I  
 Zakaly, HMH  
 Hashim, M  
 Tamam, M

### 3.3.3 Heavy metals distribution

In the present study, marine sediments from Mangrove area, Abu Tartour Harbor and Touristic Harbour were analyzed to detect the concentration and distribution of seven heavy metals (Fe, Mn, Ni, Zn, Cu, Pb and Cd) in order to understand the effect of human action and natural unputs on the quality of marine sediments and to exam the pollution situation. The mesured concentration and distribution have been listed and shown in (Table 3; and Fig. 5) ,

From the result in Table 3, we can find there is a wide range of concentrations as follow: for iron (Fe) concentration in marine sediments varies between

**Table 3:** heavy metals distribution of marine sediments at Safaga city.

	Sample name	Cu	Zn	Pb	Cd	Fe	Mn	Ni
south (Mangrove area )	S1	14	49	10	0.1	64720	490	13
	S2	12	49	20	0.0	67031	531	13
	S3	15	53	18	0.0	69343	438	15
	S4	10	38	18	0.4	71654	378	5
	S5	13	42	7	0.0	73966	398	12
	S6	12	42	24	0.0	76277	433	11
	S7	15	96	28	0.4	78589	388	7
	S8	12	57	17	0.0	80900	282	1
Abu Tartour Harbor	S9	22	117	4	1.2	83211	578	12
	S10	10	55	6	0.9	85523	333	6
	S11	11	81	18	0.6	87834	375	6
	S12	11	52	14	0.5	90146	281	5
	S13	14	51	44	0.0	92457	359	0
	S14	17	110	32	0.1	94769	620	5
north (Touristic Harbour)	S15	17	72	22	0.1	97080	307	2
	S16	10	40	25	0.0	99391	283	5
	S17	13	65	22	0.8	101703	620	4
	S18	756	361	81	0.3	104014	200	2

64720  $\mu\text{g g}^{-1}$  at South area (Mangrove area) and 104014  $\mu\text{g g}^{-1}$ (ppm) at the north area (Touristic Harbour). In the same manner magnesium (Mn) level ranges from 200  $\mu\text{g g}^{-1}$  at Touristic Harbour to 620 $\mu\text{g g}^{-1}$  at Touristic Harbour . The association of iron and manganese was well known reported that in the igneous silicate rocks, Mn is present in divalent state associated with Ferro magnesium and accessory iron minerals; [24]. There are many sources for iron and manganese transfer to the marine environment. In the present work Fe and Mn transfer to the marine environment naturally by human activation like sewage, shipment and navigation in touristic harbor. Touristic Harbour recorded the highest values compared with the other studied area due to egyptian environmental affairs agency (EEAA) allowed to use landfilling and dredging on beach and intertidal zone during construction this marina. Also there are many solid wastes and disposal of garbage from the boats in addition to, sunken boats at the area. Patch reefs and fringing reefs characterize the area in front of Tourist Harbour. Numbers of anthropogenic activities in Touristic Harbour are the main reasonable sources for the high heavy metals contents.

From the Permissible Levels of heavy metals ( $\mu\text{g g}^{-1}$ ) for Marine Sediments Quality Guidelines according to Canadian, Ontario and Florida Guidelines (Table 4) [25 - 27] we found Cu, Cd and Ni are reach The Probable Effect Level (PEL) in Quseir Harbor, while in the residual station in The Threshold Effect Level (TEL)

### 3.4 Activity Concentrations Of $^{226}\text{Ra}$ , $^{232}\text{Th}$ And $^{40}\text{K}$ In The Sediments

The activity concentrations in Bqkg-1 for  $^{226}\text{Ra}$  ( $^{238}\text{U}$ ) series,  $^{232}\text{Th}$  and  $^{40}\text{K}$  in the sediment samples under investigation were given in Table5. The activities range from  $7.4\pm 0.7$  to  $53.1\pm 3.8$  and  $6.3\pm 1.5$  to  $33.8\pm 5.2$  and  $195.7\pm 11.2$  to  $821.0\pm 46.0$  Bqkg $^{-1}$  for  $^{226}\text{Ra}$ ,  $^{232}\text{Th}$  and  $^{40}\text{K}$  respectively as it seems in Figure.7. The wide variations of the activity concentration values are due to

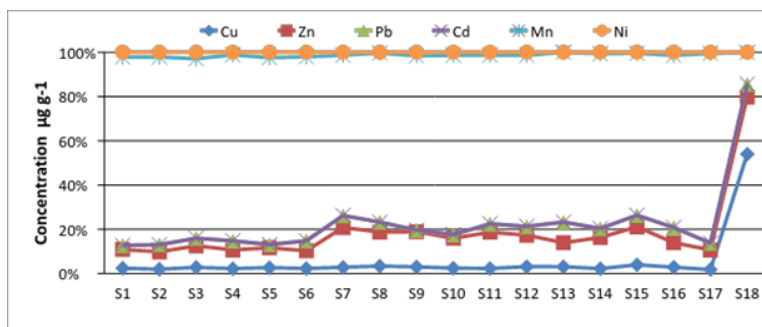


**Figure 5:** Distribution of heavy metals of marine sediments at Safaga city.

Uosif, MAM  
 Issa1, S  
 Sharma, I  
 Zakaly, HMH  
 Hashim, M  
 Tamam, M

**Table 4:** Permissible Levels of heavy metals ( $\mu\text{g g}^{-1}$ ) for Marine Sediments Quality Guidelines according to Canadian, Ontario and Florida Guidelines [25 – 27].

Metals	Levels of heavy metals ( $\mu\text{g g}^{-1}$ )		
	TEL	PEL	SEL
Cd	0.6 - 0.7	4.21	10
Cu	16 - 18.7	108	110
Ni	15.9 – 16	42.8	75
Zn	120 – 124	271	820
Pb	30.2 - 46.7	112	250
Mn	460	—	1110
Fe	20000	—	40000

**TEL:** The Threshold Effect Level, **PEL:** The Probable Effect Level, **SEL:** The Severe Effect Level

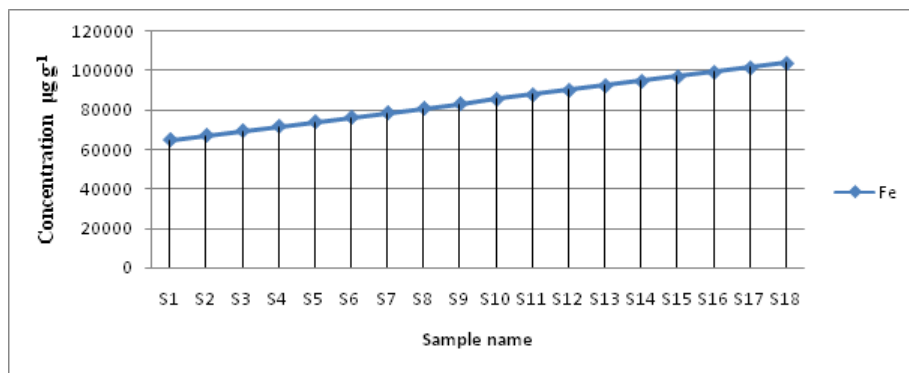


**Figure 6:** Distribution of Fe of marine sediments at Safagacity.

their presence in the marine environment and their physical, chemical and geochemical properties [28, 29]. The results show that the average activity of  $^{226}\text{Ra}$  and  $^{232}\text{Th}$  are ( $22\pm 1.7$  &  $19\pm 2.5$ ) less than the compared worldwide average value ( $35\text{Bqk}^{-1}$  for  $^{238}\text{U}$ ,  $30\text{Bqkg}^{-1}$  for  $^{232}\text{Th}$ ) while and  $^{40}\text{K}$  is higher than the compared worldwide average value ( $400\text{Bqkg}^{-1}$  for  $^{40}\text{K}$ ) of these radionuclides in the sediment (UNSCEAR, United Nations Scientific Committee on the Effects of Atomic Radiation, 2000). [30].

The main source of sediments in the beaches of the Red Sea is the terrestrial deposits transported from the fringing mountains. Uranium concentration in the shore sediment depends on the uranium concentration in the fringing mountains (crystalline rocks), also and the mobility of uranium from the rock and the shore sediment by rain and sea water, respectively [31, 32].

### 3.5 Radium Equivalent Activity Concentration Index ( $Ra_{eq}$ )

Radium equivalent ( $Ra_{eq}$ ) index in  $Bq\ kg^{-1}$  is a widely used radiological hazard index. It is a convenient index to compare the specific activities of samples containing different concentrations of  $^{226}Ra$ ,  $^{232}Th$  ( $^{228}Ra$ ) and  $^{40}K$ . It was defined on the assumption that  $10Bq\ kg^{-1}$  of  $^{226}Ra$ ,  $7\ Bq\ kg^{-1}$  of  $^{232}Th$  and  $130Bq\ kg^{-1}$  of  $^{40}K$  produce the same gamma dose rate. It was calculated as follows [33].

$$Ra_{eq} = C_{Ra} + 1.43 C_{Th} + 0.077 C_k \quad (1)$$

Where  $C_{Ra}$ ,  $C_{Th}$  and  $C_k$  are the activity concentrations of  $^{226}Ra$ ,  $^{232}Th$  and  $^{40}K$  in  $Bq\ kg^{-1}$ , respectively.  $Ra_{eq}$  was estimated for the collected samples and listed in Table 5. The values of  $Ra_{eq}$  varied from 31.5 to 140.7  $Bq\ kg^{-1}$  and the average value of  $Ra_{eq}$  was found to be 86.5  $Bq\ kg^{-1}$ . The estimated highest value of  $Ra_{eq}$  is 140.7  $Bq\ kg^{-1}$  in the present work are less than the recommended safe limit 370  $Bq\ kg^{-1}$  [34]. We use surfer 8, [35] program to describe the distribution patterns of  $Ra_{eq}$ , through figure 8 (a, b and c) we can

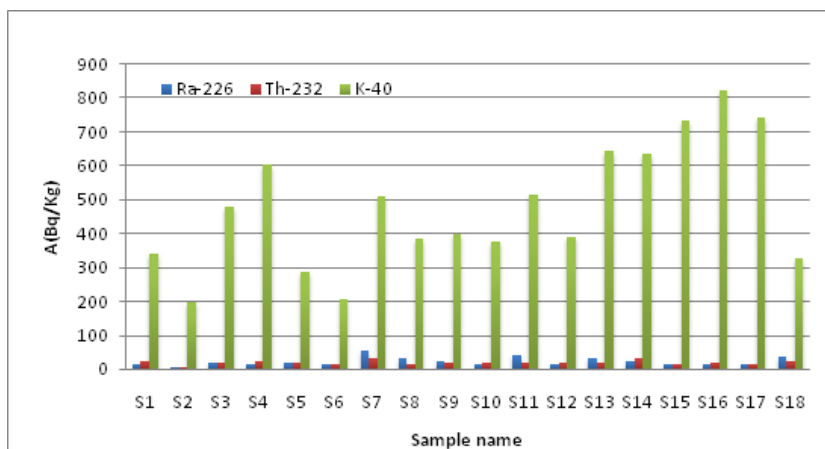


**Figure 7:** Activity concentrations of the radioelements (in  $Bq\ kg^{-1}$ ) found in studied samples.

**Table 5:** Radiological parameters in coastal sediment samples of study area.

Samples Location	Sa,Na. (Bq kg-1)	Activity concentration			R <sub>aeq</sub> (Bq kg <sup>-1</sup> )	(D <sub>r</sub> ) (nGy h <sup>-1</sup> )	(AEDE) (μSv y <sup>-1</sup> )	AGDE (μSv y <sup>-1</sup> ) (10 <sup>-6</sup> )	E <sub>LCR</sub>	H <sub>ex</sub>	H <sub>in</sub>	H <sub>l</sub>
		<sup>226</sup> Ra	<sup>232</sup> Th	<sup>40</sup> K								
S1	14.2±1.0	24.3±2.7	338.8±18.9	75	35	43	252	151	0.2	0.2	0.3	
S2	7.4±0.7	6.3±1.5	159.7±11.2	32	15	19	111	66	0.1	0.1	0.1	
S3	17.3±1.2	18.9±2.3	481.0±26.8	81	39	48	283	168	0.2	0.3	0.3	
<b>South Km 17</b>												
<b>Mangrove area</b>												
S4	13.0±1.0	22.2±4.2	604.2±33.7	91	44	54	323	190	0.2	0.3	0.3	
S5	19.3±1.3	17.3±2.0	288.2±16.1	66	31	38	222	134	0.2	0.2	0.2	
S6	14.3±1.0	13.1±1.8	206.7±20.1	49	23	28	164	99	0.1	0.2	0.2	
S7	53.1±3.8	33.8±3.3	511.2±28.5	141	66	81	466	283	0.4	0.5	0.5	
S8	31.6±3.2	14.1±1.7	386.3±21.6	81	39	48	278	167	0.2	0.3	0.3	
S9	24.1±1.5	21.1±2.4	398.3±22.5	85	40	49	288	173	0.2	0.3	0.3	
<b>Middle Abu</b>												
<b>Tartour Harbor</b>												
S10	14.7±1.1	17.8±2.0	377.6±21.3	69	33	40	238	142	0.2	0.2	0.2	
S11	42.7±2.9	16.9±1.8	515.0±28.7	106	51	63	364	219	0.3	0.4	0.4	
S12	13.8±0.9	17.6±1.8	390.4±21.8	69	33	40	239	142	0.2	0.2	0.2	
S13	31.1±3.2	19.5±2.0	643.8±37.1	109	53	64	380	226	0.3	0.4	0.4	
S14	24.5±1.8	31.9±3.3	635.1±35.4	119	57	69	409	243	0.3	0.4	0.4	
S15	14.5±0.9	15.0±2.9	735.6±41.2	93	46	56	339	197	0.3	0.3	0.3	
<b>North Touristic</b>												
<b>Harbor</b>												
S16	14.0±1.0	17.0±1.8	821.0±46.0	102	50	62	372	217	0.3	0.3	0.3	
S17	15.3±1.1	15.9±1.7	740.4±41.6	95	47	58	346	202	0.3	0.3	0.3	
S18	35.4±3.2	23.0±5.2	327.4±18.5	93	44	54	308	187	0.3	0.4	0.3	
AVERAGE		22±1.7	19±2.5	478±27.3		86	41	51	299	178	0.2	0.3
<b>Min</b>		7.4	6.3	195.7		32	15	19	111	66	0.1	0.1
<b>Max</b>		53.1	33.8	821.0		141	66	81	466	283	0.4	0.5

see the increase and decrease concentration of Raeq in mangrove area, Abu Tartor harbor and Touristic harbor, respectively.

## 4. EVALUATION OF RADIOLOGICAL HAZARD EFFECTS

### 4.1 Absorbed gamma dose rate (DR)

The contribution of natural radionuclides to the absorbed dose rate in air (DR) depends on the natural specific activity concentration of  $^{226}\text{Ra}$ ,  $^{232}\text{Th}$  and  $^{40}\text{K}$ . If a radionuclide activity is known then its exposure dose rate in air at 1 m above the ground can be calculated [36, 37]. The conversion factors used to compute absorbed gamma dose rate ( $D_R$ ) in air per unit activity concentration in Bqkg-1 (dry weight) corresponds to 0.462 nGyh-1 for  $^{226}\text{Ra}$ , 0.604 nGyh $^{-1}$  for  $^{232}\text{Th}$  and 0.0417 nGyh $^{-1}$  for  $^{40}\text{K}$ . Therefore  $D_R$  can be calculated as follows [30]:

$$D_R \text{ (nGyh}^{-1}\text{)} = 0.462 C_{\text{Ra}} + 0.604 C_{\text{Th}} + 0.0417 C_{\text{k}} \quad (2)$$

Where  $C_{\text{Ra}}$ ,  $C_{\text{Th}}$  and  $C_{\text{k}}$  are the activity concentrations of  $^{226}\text{Ra}$ ,  $^{232}\text{Th}$  and  $^{40}\text{K}$  in Bq kg $^{-1}$ , respectively. The calculated results of the absorbed dose rate in air for samples have been listed in Table 5, column 7. The absorbed dose rate values ranged between 15.3 and 65.9, with a mean value of 41.4 nGyh $^{-1}$ . This mean value is approximately the half of the world average absorbed dose rate value of 84 nGyh $^{-1}$  [38].

### 4.2 Annual effective dose equivalent (AEDE)

The annual effective dose equivalent (AEDE) outdoors in units of (mSv/ y), resulting from natural radionuclides of  $^{226}\text{Ra}$ ,  $^{232}\text{Th}$  and  $^{40}\text{K}$ . was calculated by the following formula [30].

$$\text{AEDE(mSv/y)} = D_R (0.2 * 365.25\text{d} * 24\text{h}) * (0.7 * 10^{-3}) \quad (3)$$

Where, is dose rate in (nGy/h), (0.2\*24h\*365.25d) is the outdoor occupancy time and (0.7 \* 10 $^{-3}$ ) is the conversion coefficient in Sv/Gy [39]. The annual effective dose equivalent obtained (Table 5) ranged between 18.7 and 80.8 with average value of 50.8 Svyr $^{-1}$ .(0.05mSvy $^{-1}$ ), This value about 5% of 1.0 mSvy $^{-1}$  recommended by the International Commission on Radiological Protection [40] as the maximum annual dose to members of the public[40]. Fig. 9 shows the variation of annual effective dose equivalent indifferent Samples. Also Figure 10 (a, b and c) describe the distribution patterns of AEDE, through this figure we can see the Places of Increases and decreases of AEDE in mangrove area, Abu Tartor harbor and Touristic harbor, respectively.

Uosif, MAM  
Issa1, S  
Sharma, I  
Zakaly, HMH  
Hashim, M  
Tamam, M

### 4.3 Annual gonadal equivalent (AGDE)

AGDE is a measure of the genetic significance of the yearly dose equivalent received by the population's reproductive organs (gonads) [18]. In the same context, the activity bone marrow and the bone surface cells are considered as the organs of interest by [41]. Therefore, the annual gonadal dose equivalent (AGDE) due to the specific activities of  $^{226}\text{Ra}$ ,  $^{232}\text{Th}$  and  $^{40}\text{K}$  was calculated using the following formula [42].

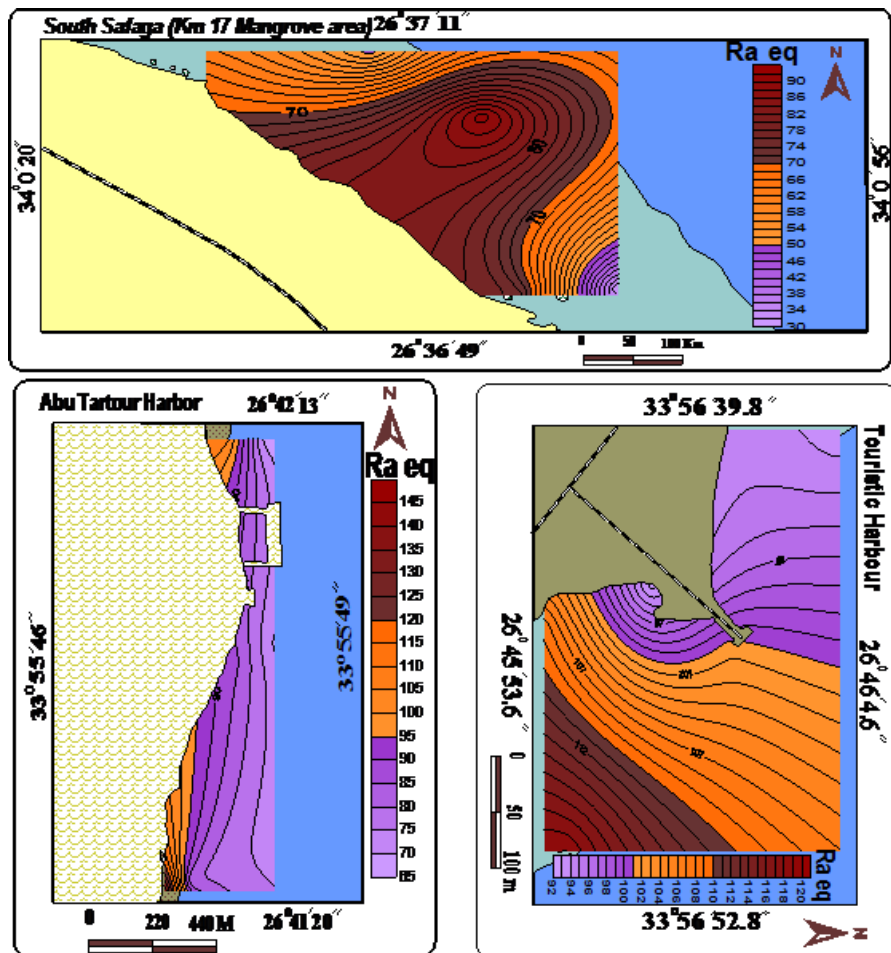
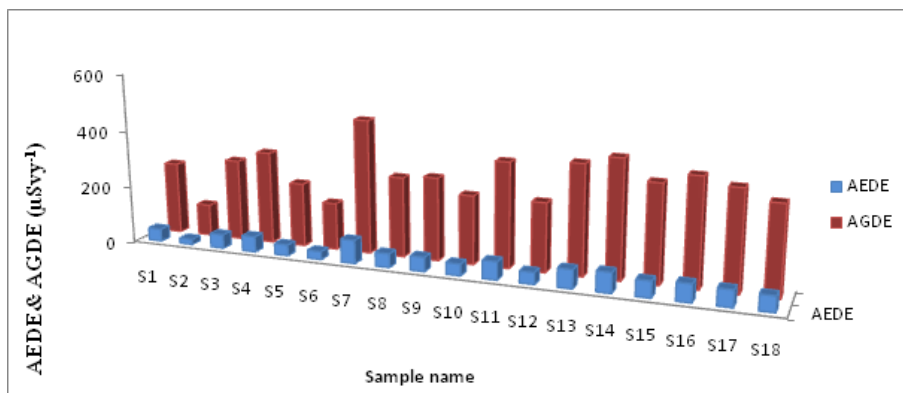


Figure 8: The distribution patterns of Raeqfor mangrove area, Abu Tartour harbor and Touristic harbor.

$$AGDR = 3.09C_{Ra} + 4.18C_{Th} + 0.314C_k (\mu\text{Svy}^{-1}) \quad (4)$$

The AGDE values are presented in Table 5. As can be seen, the average values do not, in general, exceed the permissible recommended limits, indicating that the hazardous effects of these radiations are negligible. However, the overall average values of AGDE, is found to be  $299 \mu\text{Sv y}^{-1}$ . In literature, the average value of AGDE are greater than our result and found to be  $334.3 \mu\text{Sv y}^{-1}$  for soil of Northern Jordan [43],  $282 \mu\text{Sv y}^{-1}$  for costal sediments of East costal of Tamilnadu, Inda [36],  $2398 \mu\text{Sv y}^{-1}$  for Eastern Desert of Egypt [44],  $495.5 \mu\text{Sv y}^{-1}$  for Firtina river of Turkey [45]. Fig.9 shows the samples and annual gonadal dose equivalent (AGDE).



**Figure 9:** Annual effective dose rate (AEDE) and (AGDE) ( $\mu\text{Sv y}^{-1}$ ) for sediment samples.

#### 4.4 Excess Lifetime Cancer Risk (ELCR)

Excess lifetime cancer risk (ELCR) can be defined as the excess probability of developing cancer at a lifetime due to exposure level of human to radiation. Excess lifetime cancer risk is calculated using the equation [46]: Excess lifetime cancer risk (ELCR) was calculated using the following equation and presented in Table 5.

$$\text{ELCR} = \text{AEDE} * \text{DL}(70\text{y}) * \text{Rf}(0.5\mu\text{Sv}^{-1}) \quad (5)$$

Where AEDE, DL and RF are the annual effective dose equivalent, duration of life (70 y) and risk factor ( $\text{Sv}^{-1}$ ), fatal cancer risk per Sievert. The calculated range of ELCR is  $65.5 \times 10^{-6}$  to  $282.8 \times 10^{-6}$  with an average of  $177.9 \times 10^{-6}$ .

Uosif, MAM  
 Issa1, S  
 Sharma, I  
 Zakaly, HMM  
 Hashim, M  
 Tamam, M

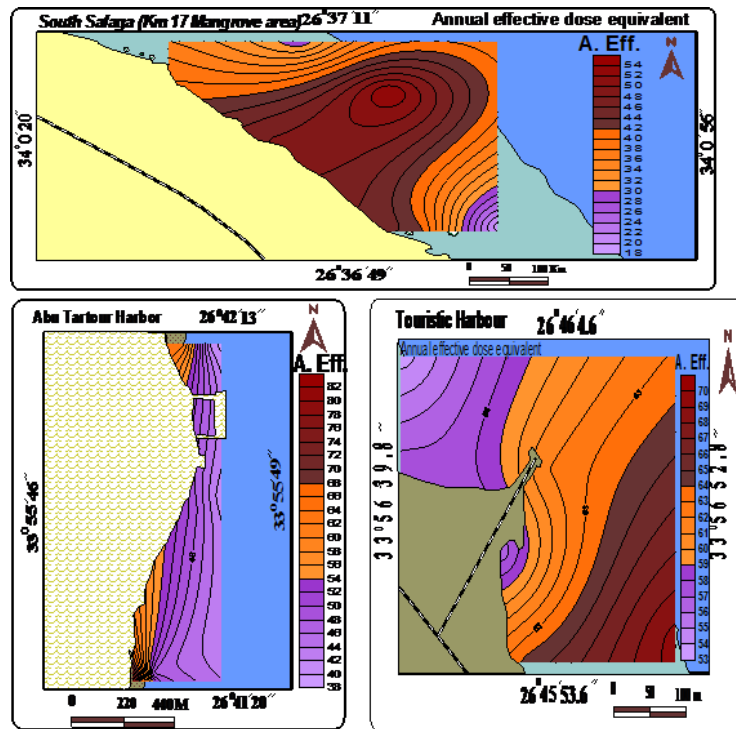


**Figure 10:** The distribution patterns of AEDE for mangrove area, Abu Tartor harbor and Touristic harbor.

The average value of ELCR from the present study area is lower than the world average ( $290 \times 10^{-6}$ ) [30]. We see from Figure 11 (a, b and c), the distribution patterns of ELCR, through this figure we can see the Places of Increases and decreases of ELCR in mangrove area, Abu Tartor harbor and Touristic harbor, respectively, Fig. 12 shows the Excess life time cancer risk (ELCR) with samples under investigation. where the highest value ( $283 \times 10^{-6}$ ) found in Abu Tartor harbor, while the lowest one ( $66 \times 10^{-6}$ ) was found in mangrove area.

#### 4.5 Calculation of Hazard Indexes

##### 4.5.1 External hazard index ( $H_{ex}$ )

The external hazard index ( $H_{ex}$ ) represents the external radiation exposure associated with gamma irradiation from radionuclides of concern. The value of  $H_{ex}$  should not exceed the maximum acceptable value of one in order to keep the hazard insignificant. The external hazard index ( $H_{ex}$ ) is defined by equation [47]:

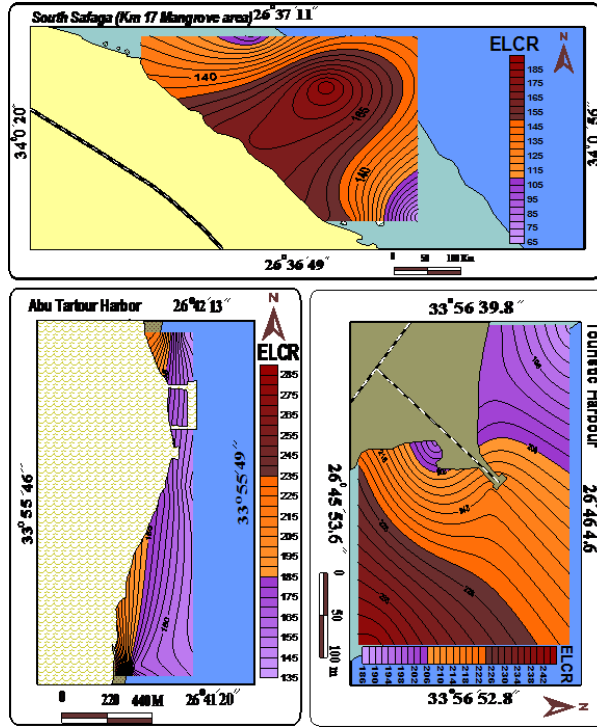


**Figure 11:** The distribution patterns of ALCR for mangrove area, Abu Tartour harbor and Touristic harbo.

$$H_{ex} = (C_{Ra} / 370 + C_{Th} / 259 + C_K / 4810) \leq 1 \quad (6)$$

Where  $C_{Ra}$ ,  $C_{Th}$  and  $C_K$  are the concentration in ( $Bq Kg^{-1}$ ) of radium, thorium and potassium respectively, Fig. 13 shows the external hazard index ( $H_{ex}$ ) with sediment samples

#### 4.5.2 Internal hazard index ( $H_{in}$ )

The internal hazard index ( $H_{in}$ ) is used to control the internal exposure to  $^{222}Rn$  and its radioactive progeny [48]. The internal exposure to radon and its daughter products is quantified by the internal hazard index ( $H_{in}$ ), which is given by the following equation [49]:

$$H_{in} = (C_{Ra} / 185 + C_{Th} / 259 + C_K / 4810) < 1 \quad (7)$$

Uosif, MAM  
 Issa1, S  
 Sharma, I  
 Zakaly, HMM  
 Hashim, M  
 Tamam, M

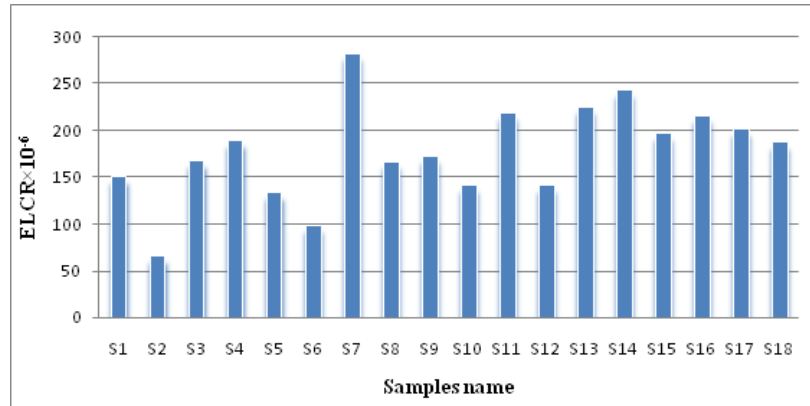


**Figure 12:** ELCR. With samples under investigation.

Where  $C_{Ra}$ ,  $C_{Th}$  and  $C_K$  are the activity concentrations of  $^{226}Ra$ ,  $^{232}Th$  and  $^{40}K$  in  $Bq\ kg^{-1}$ , respectively. The value of  $H_{in}$  must be less than the unity to have negligible hazardous effects of radon and its short-lived progeny [50], the calculated values of these indices are given in Table 5. Fig. 13 shows the internal hazard index ( $H_{in}$ ) with sediment samples.

#### 4.5.3 Gamma representative level index, ( $I_\gamma$ )

The representative level index ( $I_\gamma$ ) is used to estimate the level of  $\gamma$ -radiation hazard associated with the natural radionuclides in specific investigated samples. This index is used to correlate the annual dose rate due to the excess external gamma radiation caused by superficial materials. It is used only as a screening tool for identifying materials that might become health concerns when used as construction materials [51]. The gamma radiation hazard level of the sediment samples associated with natural radionuclides was calculated using the following formula, which was based on the radiation hazard index  $I_\gamma$ . [34]:

$$I_\gamma = (C_{Ra} / 300 + C_{Th} / 200 + C_K / 3000) \quad (8)$$

Where  $C_{Ra}$ ,  $C_{Th}$  and  $C_K$  are the specific activities ( $Bq\ kg^{-1}$ ) of  $^{226}Ra$ ,  $^{232}Th$  and  $^{40}K$ , respectively. The value of these indexes must be less than unity in order to keep the radiation hazard insignificant. The values for the representative index ranged between 0.11 and 0.47 with average value of 0.29. Values of  $I_\gamma \leq 1$  correspond to an annual effective dose of less than or equal to 1 mSv. Fig. 13 shows the Gamma representative level index ( $I_\gamma$ ) with sediment samples. From figure 13, it is clear that the highest values of  $H_{in}$ ,  $H_{ex}$  and  $I_\gamma$  have been founded in Abu Tartor harbor, while the lowest values were found in mangrove area

**Table 6:** Descriptive statistical characteristics of radioactive variables of Coastal sediment samples of Safaga city, Egypt.

Variables		<sup>226</sup> Ra	<sup>232</sup> Th	<sup>40</sup> K
N	Valid	18	18	18
	Missing	0	0	0
Mean		22.24	19.22	477.56
Std. Error of Mean		2.85	1.53	43.81
Std. Deviation		12.10	6.49	185.85
Variance		146.42	42.18	34540.97
Skewness		1.28	0.64	0.29
Std. Error of Skewness		.54	0.54	0.54
Kurtosis		1.12	1.50	-0.88
Std. Error of Kurtosis		1.04	1.04	1.04
Range		45.70	28.00	625.00
Minimum		7.40	6.00	196.00
Maximum		53.10	34.00	821.00
Frequency distribution		Log-normal	Normal	Normal

#### 4.5.4 Multivariate Statistical Analysis

##### 4.5.4.1 Descriptive statistics

Descriptive statistics is techniques that take raw scores and organize or summarize them in a form that is more manageable. Often the scores are organized in a table or a graph so that it is possible to see the entire set of scores. Even if the data set has hundreds of scores the average provides a single descriptive value for the entire data set. The list of statistical data are mean, Std. Error of Mean, Std deviation, variance, skewness, Std. Error of Skewness, kurtosis, Std. Error of Kurtosis, range, minimum, maximum, type of frequency distribution of radionuclides in sediment samples were presented in Table 7.

The spread of entire data set is analyzed by the variance and standard deviation. The shape of the distribution may also be described by skewness and kurtosis. The highest value of arithmetic mean (AM) is observed for <sup>40</sup>K (477.56 Bqkg<sup>-1</sup>) and the lowest is for <sup>232</sup>Th (19.22 Bqkg<sup>-1</sup>). The basic statistics show that the AM of activity concentrations for all samples are different from each other but are close within the SD. The values of skewness and kurtosis for <sup>40</sup>K are near to 0 and negative, respectively; therefore this radionuclide

---

Uosif, MAM  
Issa1, S  
Sharma, I  
Zakaly, HMH  
Hashim, M  
Tamam, M

---

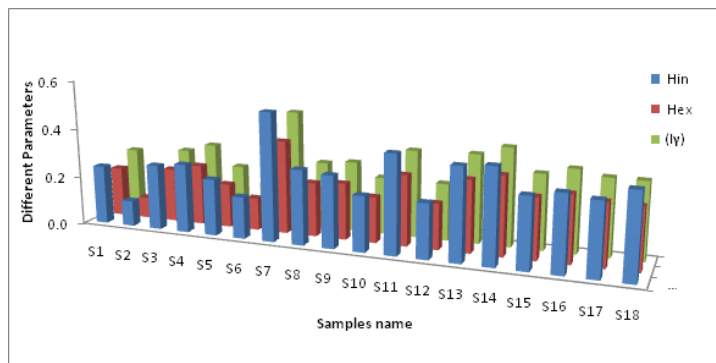


**Figure 13:** Different Parameters ( $I_{\gamma r}$ , Hex, & Hin) in sediment samples of Safaga city.

follows normal distribution. For  $^{238}\text{U}$  and  $^{232}\text{Th}$ , the skewness values are not close to the null value and kurtosis coefficient is positive, showing the non-existence of normal distribution. The positive value of kurtosis coefficient for the radionuclides indicates that distribution is higher and narrower than normal.

#### 4.6 Histograms

In statistics, a histogram is a graphical representation of the distribution of data. It is an estimate of the probability distribution of continuous variables. The frequency distribution for all radioactive variables in sediments samples were analyzed, where the histograms are given in Figs. 10-12. The graph of  $^{232}\text{Th}$  and  $^{40}\text{K}$  shows that these radionuclides demonstrate a normal (bell-shape) distribution. But  $^{238}\text{U}$  exhibited some degree of multi-modality. This multi-modal feature of the radio elements demonstrates the complexity of minerals in sediment samples.

#### 4.7 Pearson's Correlation Coefficient Analysis

Correlation analysis has been carried out, as a bivariation statistics in order to determine the mutual relationships and strength of association between pairs of variables through calculation of the linear Pearson correlation coefficient. Results for Pearson correlation coefficients between all the studied radioactive variables for sediments are shown in Table 7. The high good positive correlation co-efficient was observed between  $^{232}\text{Th}$  and  $^{226}\text{Ra}$  because radium and thorium decay series occurs together in nature [52].

**Table 7:** Pearson correlation coefficients between radioactive variables in Coastal sediment samples of Safaga city.

Variables	$^{226}\text{Ra}$	$^{232}\text{Th}$	$^{40}\text{K}$	$Ra_{eq}$	$D_R$	$H_{in}$	$H_{ex}$	AEDE	ELCR	AGDE	Gravel	Sand	Mud
$^{226}\text{Ra}$	1												
$^{232}\text{Th}$	0.541	1											
$^{40}\text{K}$	0.061	0.252	1										
$Ra_{eq}$	0.708	0.763	0.685	1									
$D_R$	0.671	0.726	0.735	0.997	1								
$H_{in}$	0.859	0.740	0.517	0.970	0.955	1							
$H_{ex}$	0.708	0.763	0.684	0.999	0.997	0.970	1						
AEDE	0.671	0.726	0.735	0.997	1	0.955	0.997	1					
ELCR	0.671	0.726	0.735	0.997	1	0.955	0.997	1	1				
AGDE	0.634	0.706	0.770	0.992	0.999	0.938	0.992	0.999	0.999	1			
Gravel	0.162	0.045	0.115	0.159	0.161	0.171	0.159	0.161	0.161	0.160	1		
Sand	0.128	0.043	0.089	0.127	0.129	0.137	0.127	0.129	0.129	0.128	-0.983	1	
Mud	0.197	0.015	0.151	0.184	0.190	0.202	0.184	0.190	0.190	0.189	-0.191	0.007	1

Density Functional  
Theory Study  
of Structural  
and Electronic  
Properties of Group  
V Transition Metal  
Carbide

Uosif, MAM  
 Issa1, S  
 Sharma, I  
 Zakaly, HMMH  
 Hashim, M  
 Tamam, M

**Table 8:** Pearson correlation coefficients between radioactive variables and heavy metals in Coastal sediment samples of Safaga city.

	<i>Ra-226</i>	<i>Th-232</i>	K-40	Cu	Zn	Pb	Cd	Fe	Mn	Ni
<sup>226</sup> Ra	1									
<sup>232</sup> Th	0.541	1								
<sup>40</sup> K	0.061	0.252	1							
Cu	0.275	0.153	-0.200	1						
Zn	0.422	0.313	-0.137	0.952	1					
Pb	0.393	0.241	0.103	0.833	0.798	1				
Cd	0.104	0.128	0.047	-0.007	0.142	-0.268	1			
Fe	0.203	0.102	0.586	0.399	0.462	0.524	0.220	1		
Mn	-0.215	0.115	0.009	-0.412	-0.262	-0.350	0.212	-0.243	1	
Ni	-0.303	-0.111	-0.525	-0.271	-0.272	-0.479	-0.040	-0.756	0.478	1

The positive correlation coefficient was absorbed between <sup>226</sup>Ra, <sup>232</sup>Th and <sup>40</sup>K with all the radiological parameters. This implies that, there is a very strong relationship between the radionuclides in sediments and radiological parameters. Hence this strong relationship shows the all three radionuclides contribute the emission of gamma radiation in all the samples. Also we see weak correlation between radionuclides in sediments (gravel and sand), while increase with mud. As it appear from table 7.

Correlation coefficients between heavy metals and radioactivity were determined. Natural radioactivity in the studied area originated from the costal sediments samples. Spearman correlation coefficients between heavy metals and activity concentrations of natural radioactive isotopes are presented in Table 8. Significant negative correlation between radioactivity and Ni is seen (the correlation coefficient R for all data pairs is between -0.111 and -0.525). In Table 8 that significant positive correlations occur between Natural radioactivity and Pb, Cd and Fe.

#### 4.8 Cluster Analysis

Cluster analysis (CA) is one of multivariate techniques used to identify and classify groups with similar characters in a new group of observations. Each observation in a cluster is most like others in the same cluster. Similarity is a measure of distance between clusters relative to the largest distance between any two individual variables [53]. The zero distance means the clusters are

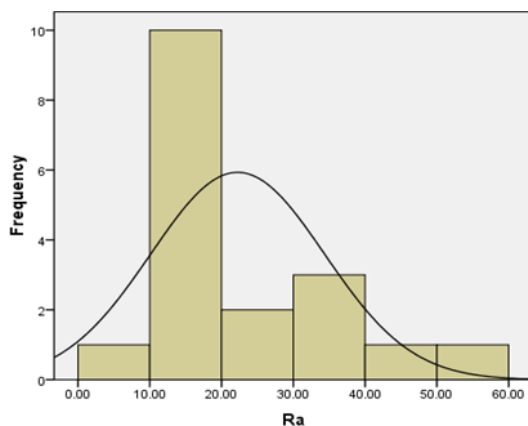


**Figure 14:** Frequency distribution of  $^{226}\text{Ra}$ .

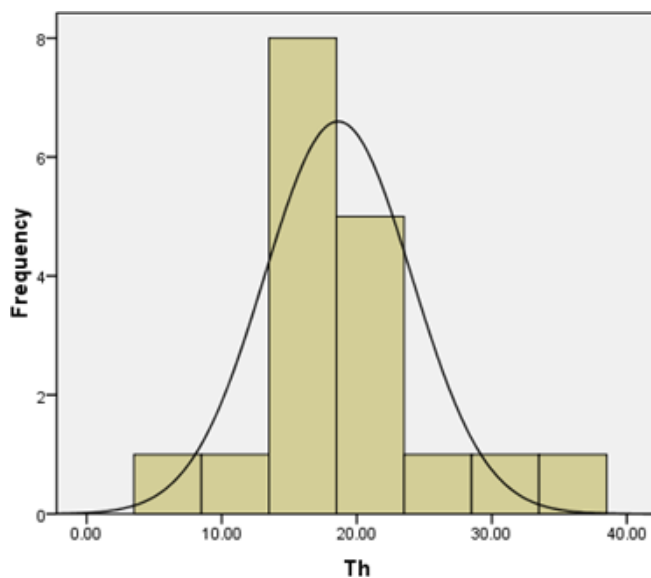


**Figure 15:** Frequency distribution of  $^{232}\text{Th}$ .

100% similarity in their sample measurements, whereas the cluster areas are as disparate as the least similar region means similarity of 0%. Cluster analysis was carried out through axes was to identify similar characteristics among natural radioisotopes and radiological parameters in the sediments.

Uosif, MAM  
 Issa1, S  
 Sharma, I  
 Zakaly, HMM  
 Hashim, M  
 Tamam, M

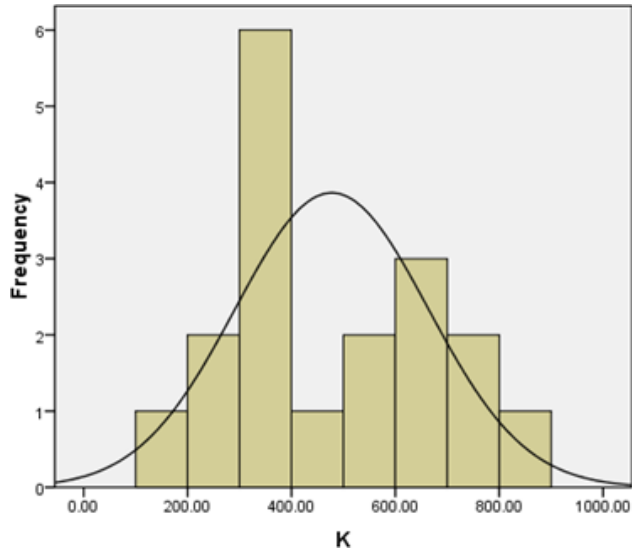


**Figure 16:** Frequency distribution of  $^{40}\text{K}$ .

Dendrogram using Average Linkage (Between Groups)

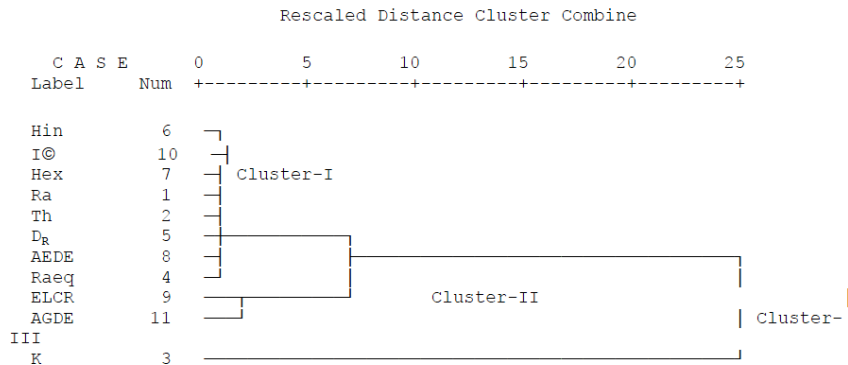


**Figure 17:** Dendrogram shows the clustering of radionuclides.

In CA, the average linkage method along with correlation coefficient distance was applied and the derived dendrogram shown in Fig. 13. In this dendrogram, 8 radiological parameters and three radionuclides were grouped into three statistically significant clusters. Cluster-I consist of  $H_{in}$ ,  $I\gamma$ ,  $H_{ex}$ ,  $^{226}\text{Ra}$ ,  $^{232}\text{Th}$ ,  $D_R$ , AEDE and  $Ra_{eq}$ . Cluster-II consists of ELCR and AGDE. Cluster-III separately accounted for  $^{40}\text{K}$ . From this cluster analysis, external hazard index,

---

internal hazard index and Gamma representative level index in the study area are due to the concentration of  $^{226}\text{Ra}$  and dose absorbed by the human beings are due to high concentration of  $^{232}\text{Th}$ . Cluster-III suggests that  $^{40}\text{K}$  does not contribute to any radiological parameters in the study area.

Density Functional  
Theory Study  
of Structural  
and Electronic  
Properties of Group  
V Transition Metal  
Carbide

---

## CONCLUSIONS

The conclusion of our study can be summarized in the following points:

1. The results show that the average activity of  $^{226}\text{Ra}$  and  $^{232}\text{Th}$  are less than the compared worldwide average while  $^{40}\text{K}$  is higher than the compared worldwide average value of these radionuclides in the sediment [30].
2. Mangrove area and Abu Tartour Harbor recorded the highest values of organic matter content compared with Touristic Harbour. The high content of the organic matter in tidal flat sediments to the terrigenous flux. Also, they recorded that the terrestrial materials rich in organic matter and the high organic productivity are the two main reasons for the higher organic matter content.
3. Sediments sampled in Safaga Harbour and Touristic harbor were recorded the highest values of Fe, Zn, Pb and Cd when compared with Mangrove area. The high concentrations of these metals may be caused by anthropogenic activities. The main factor is phosphate and bauxite. This is attributed to the high input of terrigenous fragments including mafic minerals and the packing of cement in Safaga Harbour
4. The presence of the heavy metals detected in both soil profiles allows us to conclude that the pollution was produced a long time ago and the pollutant activities in the investigated areas are still present

## ACKNOWLEDGEMENTS

This work was carried out using the nuclear analytical facilities at Physics Department, Faculty of Sciences, Al-Azhar University, Assiut, Egypt. And analytical facilities National Institute of Oceanography and Fisheries, Red Sea Branch.

## REFERENCE

- [1] A. I. Beltagy, and KH. A. Mousa, Bull. Inst. Oceanogr. and Fish., Egypt, 10: 99-109 (1984).
- [2] A. Kurnaz, et al., Appl. Radiat. Isot65, 1281–1289 (2007).  
<http://dx.doi.org/10.1016/j.apradiso.2007.06.001>

---

Uosif, MAM  
Issa1, S  
Sharma, I  
Zakaly, HMM  
Hashim, M  
Tamam, M

---

- [3] A. M. Mansour, A. H. Nawar, and A W. Mohamed, *Sedimentology of Egypt*, 8: 231-242 (2000).
- [4] A. M. Mansour, A. H. Nawar, and A. M. Mohamed, *Egyptian Jour. of Geo.* 41/2A: 239-272 (1997).
- [5] A. Sanchez-Cabeza, M. Ortega, J. Merino, and P. Masque, *J. Mar. Syst.* 33–34, 457–472. (2002). [http://dx.doi.org/10.1016/S0924-7963\(02\)00071-4](http://dx.doi.org/10.1016/S0924-7963(02)00071-4)
- [6] A. Strezov, M. Yordanov, M. Pimpl, T. Stoilova, *Journal of Health Physics* 70 (1), 70–80 (1996). <http://dx.doi.org/10.1097/00004032-199601000-00011>
- [7] A.M. Mansour, *Sedimentology of Egypt*. V. 7: 25-36 (1999).
- [8] C. E. Rossler, Z. A. Smith, W. E. Bolch, and R. J. Prince, *Journal of Health Physics*, 37, 269–277(1979).  
<http://dx.doi.org/10.1097/00004032-197909000-00001>
- [9] D. D. MacDonald, et al., *Ecotoxicology*, 5: 253-278 (1996).  
<http://dx.doi.org/10.1007/BF00118995>
- [10] D. Persaud, R. Jaagumagi, and A. Hayton, *The provincial sediment quality guidelines*. Ontario Ministry of the Environment (1990).
- [11] El-Sayed, M. Kh., (1984). Reefal sediments of Al-Ghardaqa, Northern Red Sea Egypt. *Mar. Geol.*, 56: 259-271.
- [12] El-Taher and M A M Uosif, *J. Phys. D: Appl. Phys.* 39, 4516–4521(2006).  
<http://dx.doi.org/10.1088/0022-3727/39/20/032>
- [13] G. Suresh, et al., *Applied Radiation and Isotopes*, 69, 1466-1474 (2011).  
<http://dx.doi.org/10.1016/j.apradiso.2011.05.020>
- [14] GENIE-2000 Basic Spectroscopy (Standalone) V1.2A Copyright (c) (1997), Canberra Industries.
- [15] H. A. Al-Trabulsy, A. E. Khater, and F.I. Habbani, *Radiation Physics and Chemistry* 80: 343–348 (2011).  
<http://dx.doi.org/10.1016/j.radphyschem.2010.09.002>
- [16] H. E. Heldal, P. Varskog, and L. FØyn, *Sci. Total Environ.* 293, 233–245 (2002).  
[http://dx.doi.org/10.1016/S0048-9697\(02\)00041-4](http://dx.doi.org/10.1016/S0048-9697(02)00041-4)
- [17] H.A. Madkour, Ph.D. Thesis, South Vally Univ., Qena p 317 (2004).
- [18] Hashem A. Madkour, Ahmed W. Mohammed, *Environ Geol.* 54:257–267(2008).  
<http://dx.doi.org/10.1007/s00254-007-0813-8>
- [19] I. F. Al-Hamarneh, M. I. Awadallah, *Radiat. Meas.* 44, 102–110 (2009).  
<http://dx.doi.org/10.1016/j.radmeas.2008.11.005>
- [20] I. Tanaskovic, D. Golobocanin and N. Miljevic, *Journal of Geochemical Exploration*, 112, 226-234. (2012).  
<http://dx.doi.org/10.1016/j.gexplo.2011.08.014>
- [21] IAEA-314: 226Ra, Th and U in Stream Sediment, Vienna, Austria, (1991)
- [22] ICRP, (1993). ICRP Publication 65. Ann. ICRP 23(2). Pergamon Press
- [23] ICRP-60, (1990) Recommendations methods. Part 1. Monoenergetic sources of natural radionuclides in the ground, GSF-B2/90 of the ICRP. Oxford: Pergamon Press
- [24] J. B. Bennet, and J. Cubbage, (1991). *Summary of Criteria and Guidelines for Contaminated Freshwater Sediments*. Washington State Department of Ecology, Olympia, WA PMCid:PMC1004336
-

- 
- [25] J. Beretka, P.J. Mathew, *Health Physics* 48, 87–95 (1985).  
<http://dx.doi.org/10.1097/00004032-198501000-00007>
- [26] James, P. M., Cambridge University Press. Cambridge, 3/5, p. 229(1991).  
 Jr EW. Dean, *J Sediment Petrol.*; 44, 242–248 (1974).
- [27] K. Mamont-Ciesla, B. Gwiazdowski, M. Biernacka, and A. Zak, special symposium on natural radiation environment; Bombay (India); 19-23 Jan (1981)
- [28] M. A. M. Uosif, A. El-Taher and G. E. Abbady, *Radiation Protection Dosimetry*, 131, 331e339 (2008).
- [29] M. A. M. Uosif, Mahmoud Tammam, Shams A. M. Issa and Reda Elsaman, *International Journal of Advanced Science and Technology* 42, 69-81. (2012)
- [30] M. Brenner, MW. Binford, *Can J Fish Aquat Sci.*; 45, 294–300 (1988).  
<http://dx.doi.org/10.1139/f88-035>
- [31] M. H. El Mamoney, A. E. M. Khater, *J. Environ. Radioact.* 73, 151–168 (2004).  
<http://dx.doi.org/10.1016/j.jenvrad.2003.08.008>
- [32] M. H. El Mamoney, A. E. Rifaat, *J. King Abdulaziz Univ. Marine Sciences* 12, 149–160 (2001).
- [33] M. Jankovic, D.Todorovic, and M. Savanovic, *Radiation Measurements*, 43: 1448-1452 (2008).  
<http://dx.doi.org/10.1016/j.radmeas.2008.03.004>
- [34] M. SureshGandhi, et al., *Journal of Radiation Research and Applied Sciences*, 7: 7-17 (2014). <http://dx.doi.org/10.1016/j.jrras.2013.11.001>
- [35] MAM Uosif, Madkour Hashim, Shams Issa, Mahmoud Tamam and Hesham M. Zakaly., *International Journal of Advanced Science and Technology*, 86:9-30 (2016).
- [36] Mohamed Amin Mahmoud Uosif, *SDU Journal of Science (E-Journal)*, 6 (2): 120-126 (2011).
- [37] N. N. Jibiri, I. C. Okeyode, *Radiat. Phys. Chem.* 81, 103–112 (2012).  
<http://dx.doi.org/10.1016/j.radphyschem.2011.10.002>
- [38] P. G. Jeffery, *Chemical methods of rock analysis*. 2nd ed., pergamon press, Oxford, 525p (1975).
- [39] R. Chester, F. G. Lin, A. S. Basaham, *Geol. Soc. London* 151, 351–360 (1994).  
<http://dx.doi.org/10.1144/gsjgs.151.2.0351>
- [40] R. E. Carver, John Wiley and Sons, p. 653 (1971).
- [41] R. Krieger, *Betonwerk Fertigteile* Tech 47,468–473 (1981).
- [42] R. Ravisankar, et al., *Radiat. Phys.Chem.*81, 1789–1795(2012).  
<http://dx.doi.org/10.1016/j.radphyschem.2012.07.003>
- [43] R. Ravisankar, et al., *Radiation Physics and Chemistry* 103, 89-98 (2014).  
<http://dx.doi.org/10.1016/j.radphyschem.2014.05.037>
- [44] S. A. Khatir, et al., *Mar. Pollut. Bull.* 36, 19–26 (1998).  
[http://dx.doi.org/10.1016/S0025-326X\(98\)90025-X](http://dx.doi.org/10.1016/S0025-326X(98)90025-X)
- [45] S. U. El-Kameesy, et al., *Turk. J. Eng. Environ. Sci.*32, 245–251 (2008).
- [46] Shams AM. Issa, AMA Mostafa, and Abd El-Salam M Lotfy, *Journal of Radioanalytical and Nuclear Chemistry*, 303: 53-61(2015).

---

Uosif, MAM  
Issa1, S  
Sharma, I  
Zakaly, HMM  
Hashim, M  
Tamam, M

---

- [47] Shams ISSA, Mohamed UOSIF and Reda ELSAMAN, Turkish J Eng Env Sci, 37: 109 – 122 (2013)
- [48] SM. Flannery, DR. Snodgrass, JT. Whitmore, Hydrobiologia. 92, 597–602 (1982). <http://dx.doi.org/10.1007/BF02391974>
- [49] Surfer Version 8.00 - Feb 11 (2002) Surface Mapping System Copyright 1993-2002, Golden Software, Inc.
- [50] UNSCEAR, (1988). Sources, Effects and Risks of Ionizing Radiation. United Nations, New York.
- [51] UNSCEAR, (2000). Exposures from natural radiation sources. UNSCEAR Report. United Nations.
- [52] W. Arafa, J.Environ.Radioact.75,315–327 (2004). <http://dx.doi.org/10.1016/j.jenvrad.2004.01.004>